DOI: 10.1002/chem.200902761

Combination of Cobalt and Iron Polypyridine Complexes for Improving the Charge Separation and Collection in Ru(terpyridine)$_2$-Sensitised Solar Cells

Stefano Caramori,*[a] Jérôme Husson,[c] Marc Beley,[b] Carlo A. Bignozzi,[a] Roberto Argazzi,[d] and Philippe C. Gros*[b]

Abstract: Mixtures of polypyridine Fe^{II} and Co^{II} complexes are used as electron mediators in Ru–thienyltpy-sensitised solar cells (tpy = terpyridine). The use of the metalorganic redox couples allows for improved charge-collection efficiency with respect to the classical iodide/iodine couple which, when associated to Ru–tpy$_2$ dyes, usually produces poor performance. The improved charge collection is explained by a combination of effective dye regeneration and decreased recombination with the oxidised electrolyte on the basis of data obtained by transient spectroscopy and photoelectrochemical measurements. The efficiency of the regeneration cascade is also critically dependent upon the ability of the Co^{II} complex to intercept Fe^{III} centres, as clearly indicated by chronocoulometry experiments.

Keywords: cobalt · electron collection · iron · recombination · solar cells

Introduction

The huge amount of work focusing on dye-sensitised solar cells (DSCs) attests to their attractiveness as cost-effective alternatives to silicon-based photovoltaic devices.[1] The principle of these DSCs is to harvest photons from sunlight using a dye, usually a ruthenium-based complex with a broad absorption band, linked by electron-withdrawing groups (generally carboxylic acids) to a photoanode (a conducting fluorine-doped tin oxide (FTO) glass covered by a film of nanocrystalline TiO_2). The absorbed photons induce excitation of the metal centre by a metal-to-ligand charge transfer (MLCT) transition and subsequent electron injection into the TiO_2 conduction band (CB). A redox mediator is then employed to regenerate the dye in its reduced ground state by electron donation. The oxidised form of the mediator is then restored by reduction at the cathode, thus completing the electric circuit.

When examined in detail, the operating scheme is not as simple as described above, and many elements and factors have to be understood and thus controlled to obtain optimal performances of the DSC.

The redox mediator is a key element of the device. Indeed, it must ensure a very fast regeneration of the dye ground state (namely Ru^{II}) to avoid back recombination with TiO_2 conduction band electrons which, in the absence of kinetic barriers, can also recombine with the oxidised form of the mediator. All these recombination processes generate dark currents and may dramatically reduce the cell performance.

The best, and still most used, system is the I^-/I_3^- couple,[2] which normally exhibits ideal electron-transfer kinetics for the functioning of the DSC.[3] However, this mediator is not without drawbacks:

1) I_3^- absorbs light in the visible region and can compete with the dye for light harvesting.
2) If metal collectors have to be used to improve the electron-collection efficiency, the corrosivity of I^-/I_3^- may affect long-term cell stability.[3]

[a] Dr. S. Caramori, Prof. C. A. Bignozzi
Dipartimento di Chimica, Università di Ferrara
Via Luigi Borsari 46, 44100 Ferrara (Italy)
Fax: (+39) 5-32-24-07-09
E-mail: cte@unife.it

[b] Prof. M. Beley, Dr. P. C. Gros
SRSMC-CNRS, Nancy Université
Boulevard des Aiguillettes, 54506 Vandoeuvre-Lès-Nancy (France)
Fax: (+33) 3-83-68-47-85
E-mail: philippe.gros@srsmc.uhp-nancy.fr

[c] Dr. J. Husson
Institut UTINAM, UMR 6213, Université de Franche Comté
16 Route de Gray, 25030 Besançon (France)

[d] Dr. R. Argazzi
Istituto per la Sintesi Organica e la Fotoreattività (ISOF-CNR)
c/o Chemistry Department
Via Luigi Borsari 46, 44100 Ferrara (Italy)

Supporting information for this article is available on the WWW under http://dx.doi.org/10.1002/chem.200902761.

3) The ability of such electron relays to interact (or react) with substituents on the dye ligands has recently been observed: I_3^- can form an ion pair with the dye cation,[4] thus favouring the back-recombination process by proximity effects.

Thus, the search for alternatives to I^-/I_3^- has become an interesting challenge for both fundamental and practical reasons, and may influence the future development of DSCs. At present, one of the most promising routes is the use of bulky cobalt complexes as monoelectronic transfer mediators (a two-electron process is necessary for I^-/I_3^-). The advantages of these complexes are a very weak absorption in the visible region and the possibility of tuning their redox potential by modifying their coordination sphere, to adapt them to a wider range of ruthenium dyes. Valuable photovoltaic performance has been obtained by using the $[Co(dbbip)_2]^{2+}/[Co(dbbip)_2]^{3+}$ couple [dbbip = bis(1′-butylimidazol-2′-yl)pyridine].[3,5] Another alternative is the $[Co(dtb)_3]^{2+}/[Co(dtb)_3]^{3+}$ (dtb = 4,4′-di-*tert*-butyl-2,2′-bipyridine)[6,7] couple. Cobalt–polypyridine complexes are generally kinetically slow electron donors and their performances can be improved when used in conjunction with some auxiliary couples, named co-mediators, intended to accelerate the dye regeneration.[8,9] These metalorganic mediators were found to be not corrosive towards most common metals, and their easy preparation from commercially available ligands makes them potentially suitable for large-scale production.[9]

Another possible strategy to improve cell stability is the wiring of a hole transporter to the sensitiser, to thus have, ideally, a solid-state device, and thus addressing issues related to cell sealing and leaking, which are encountered when liquid electrolytes are used. This has been realised by binding polypyrroles[10] or oligo-[11,12] and polythiophene[13] to ruthenium polypyridine complexes. Unfortunately, poor photovoltaic performances were obtained due to recombination and slow hole transport into the polymer backbone.[12,14] Additionally, calculations have shown that the attachment of the thienyl group to terpyridine in Ru–tpy-based dyes tends to localise the LUMO orbitals on this ligand and not on the terpyridine bearing the electron-attracting transferring group (e.g., carboxylic group), thus disfavouring electron injection into the TiO_2 conduction band.[10,12,14] These bis-terpyridine-based sensitising agents are, however, more attractive than the bipyridine-based ones in terms of preparation (only two ligands have to be coordinated to the metal) and geometry control, because the $[Ru(tpy)_2]^{2+}$ complexes have a linear morphology allowing vectorial electron transport. The photovoltaic performances of the family of $[Ru(tpy)_2]^{2+}$ dyes have been evaluated only by using the I^-/I_3^- mediator, and their resulting performances were quite poor. This has sometimes been attributed to their low charge injection quantum yield.[15]

Herein, we report that the use of mediators based on cobalt complexes associated with adequate co-mediators based on iron complexes result in an interesting improvement of the photovoltaic performance of thienyl-containing $[Ru(tpy)_2]^{2+}$ dye **5** (Scheme 1). Kinetic studies on dye regeneration and recombination as well as electrochemical and photoelectrochemical experiments have been performed to explain such a mediator effect.

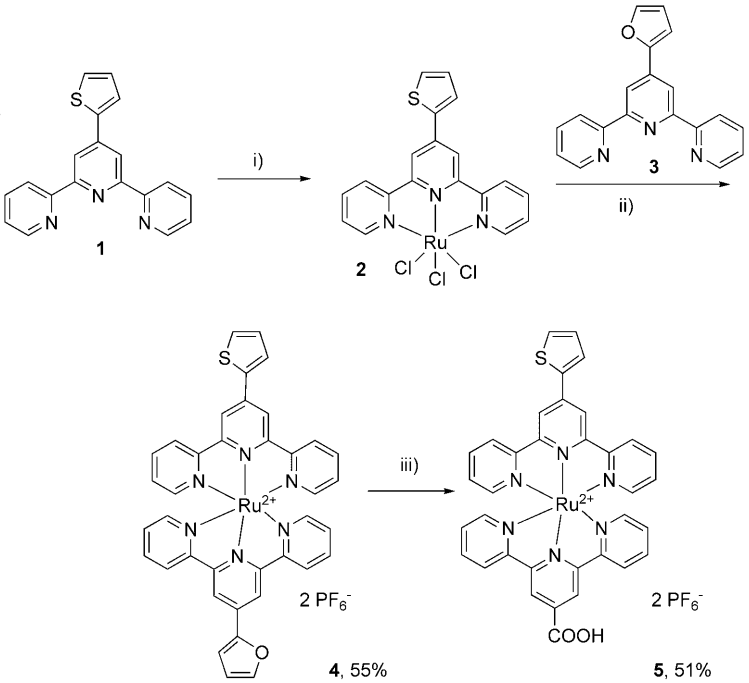

Scheme 1. Preparation of dye **5**. i) $RuCl_3{\cdot}3H_2O$ (1 equiv), absolute ethanol, reflux, 3 h. ii) 1) $AgBF_4$, DMF, reflux, 3 h. 2) **3** (1 equiv), DMF, reflux, 3 h. 3) sat. aq KPF_6. iii) $KMnO_4$, CH_3CN/H_2O (1:1), KOH (pH 14), RT, 24 h, then HCl (pH 3).

Results and Discussion

Dye **5** was synthesised by first reacting thienylterpyridine **1** with $RuCl_3{\cdot}xH_2O$ in DMF, which led to the trichloro complex **2**. Ruthenium complex **4** was obtained in good yield after dechlorination of **2** by use of $AgBF_4$ and subsequent coordination with the furylterpyridine **3**. The carboxylic group was generated by oxidation of the furyl group of **4** with $KMnO_4$, thus providing dye **5** in 51% yield (Scheme 1).

UV/Vis and electrochemical properties of **5** were in agreement with those of $[Ru(tpy)_3]^{2+}$ complexes (Table 1). Several bands of high intensity were present in the UV region, corresponding to π–π* transitions, and one band of medium intensity in the visible region with a maximum absorption value at 490 nm ($\varepsilon = 2.4\times10^4\,M^{-1}cm^{-1}$) was due to the MLCT transition. The cyclic voltammogram indicated that the Ru^{II}/Ru^{III} couple was oxidised reversibly at 1.20 V versus SCE.

The UV/Vis transient spectra obtained following 532 nm laser excitation of **5** in solution (CH_3CN) and chemisorption on a thin transparent TiO_2 film are shown in Figure 1.

The transient difference absorption spectrum in solution shows the typical features of a short-lived (9 ns, from monoexponential fitting of the transient absorption) triplet

Table 1. Photophysical and electrochemical properties of dye **5**.

$\lambda_{abs\text{-}max}$ [nm] ($\varepsilon \times 10^{-4}$ [$M^{-1}cm^{-1}$])[a]	490 (2.4), 312 (5.4), 275 (5.7), 231 (5.1)
$\lambda_{em\text{-}max}$ [nm][b]	660
$E_{1/2}$ Ru^{III}/Ru^{II} [V versus SCE] (ΔE_p [mV])[c]	1.20 (70)
ligand processes [V versus SCE] (ΔE_p [mV])[d]	−1.25 (100), −1.47 (100)

[a] Measured in CH_3CN at 25 °C. [b] $\lambda_{excit} = 490$ nm, OD < 0.05 in the absence of O_2. [c] First oxidation potential standardised with Fc^+/Fc (Fc^+/Fc = ferrocenium/ferrocene) as internal standard and converted into the SCE scale by adding 0.33 V ($E_{1/2}$ Fc^+/Fc); recorded at 100 mV s^{-1}; $LiClO_4$ used as supporting electrolyte. [d] First reduction potential, the value representing $E_{1/2}$ L/L^-.

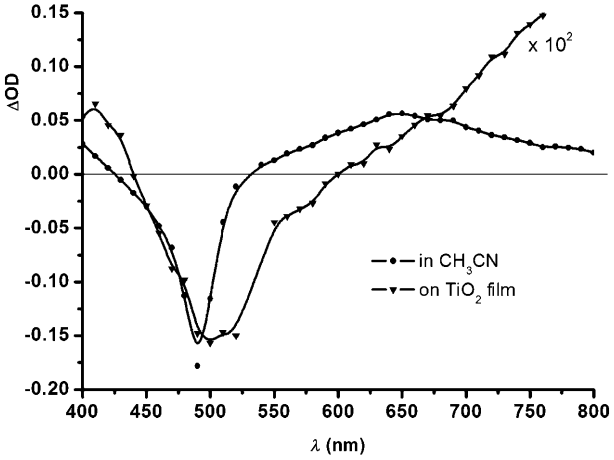

Figure 1. Differential transient absorption spectra of **5** in CH_3CN solution and on TiO_2 film.

MLCT excited state. It consists of a moderate absorption in the UV region, followed by sharp ground-state bleaching (490 nm) and by a broad absorption extending at longer wavelengths up to the IR range, with a maximum at 630 nm, resulting mainly from reduced ligand-localised transitions. On TiO_2, the spectroscopic signature was entirely different, because it resulted from the formation of the charge-separated state Ru^{III}–e^-(CB-TiO_2), following the laser-induced charge injection. The Ru^{III} bleach is shifted to 510 nm, in agreement with the ground-state absorption spectrum on TiO_2. The intense absorption at long wavelengths is dominated by the dye cation absorption. The formation of the charge-separated state was instrument-response limited, setting a lower value for the charge-injection rate constant of 1.5×10^8 s^{-1}. The decay of the charge-separated state due to Ru^{III}–e^-(CB-TiO_2) recombination follows a marked multiexponential kinetic and, at our excitation energy density (≈ 3 mJ cm^{-2} $pulse^{-1}$), is 90% complete within 2 μs from the laser pulse. Thus, $\tau_{2/3}$, corresponding to the time at which two-thirds of the maximum signal amplitude is recovered, is 84 ns.

A set of DSCs consisting of **5** as dye and four different types of redox mediators were comparatively evaluated. In particular, besides the classical I^-/I_3^- system, electron mediators based on the $[Co(dtb)_3]^{2+}/[Co(dtb)_3]^{3+}$ (CoDTB) couple associated to the iron-based co-mediators $[Fe(dmb)_3]^{2+}/[Fe(dmb)_3]^{3+}$ (FeDMB) and $[Fe(dmob)_3]^{2+}/[Fe(dmob)_3]^{3+}$ (FeDMOB) were examined.

The iron co-mediators usually give rise to fast electron-transfer reactions, due to their small inner sphere reorganisation energy and have been used to kinetically improve the regeneration of the dye. The redox potentials ($E_{1/2}^{3+/2+}$) of FeDMB and FeDMOB are 0.85 and 0.75 V

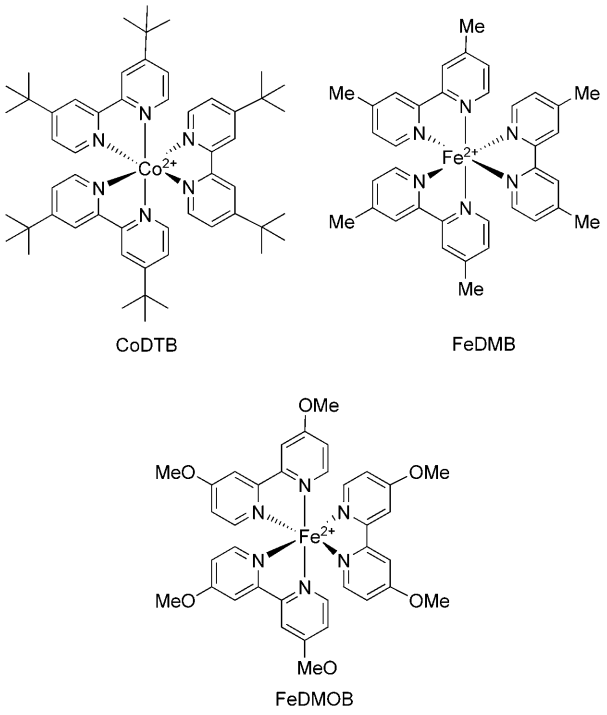

versus SCE, respectively. Because the half-wave potential of CoDTB is 0.22 V and that of **5** is 1.20 V versus SCE, the potentials of the iron complexes are ideally positioned to act as a relay by firstly reducing the photooxidised dye. Subsequently, the oxidised co-mediators $FeDMB^{3+}$ or $FeDMOB^{3+}$ can be intercepted rapidly by $CoDTB^{2+}$, preventing their direct charge recombination at the TiO_2 surface.[9] Thanks to its electrochemical inertness towards conduction band electrons (in contrast with Fe^{3+} species), the formed $CoDTB^{3+}$ gives rise to minimal recombination with conduction band electrons and diffuses freely to the counter electrode, where its reduction to Co^{II} is catalysed by suitable gold or platinum layers (Figure 2). Co/Fe ratios of 10:1 were used to ensure an improvement in dye regeneration, while keeping the stationary Fe^{III} concentration low enough to minimise its direct recombination at the TiO_2 interface.

The incident photon-to-current efficiency (IPCE) measurements (Figure 3) revealed a striking effect of the CoDTB/FeDMB mediator, resulting in 65% maximum IPCE. As already observed for similar thienyltpy-based dyes, I^-/I_3^- gave a poor performance with only 20% IPCE. The two other systems, CoDTB alone and the CoDTB/

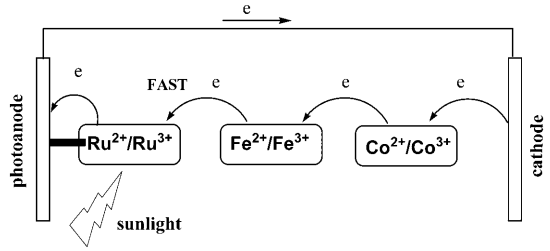

Figure 2. The role of the iron-based co-mediator in accelerating oxidised dye reduction.

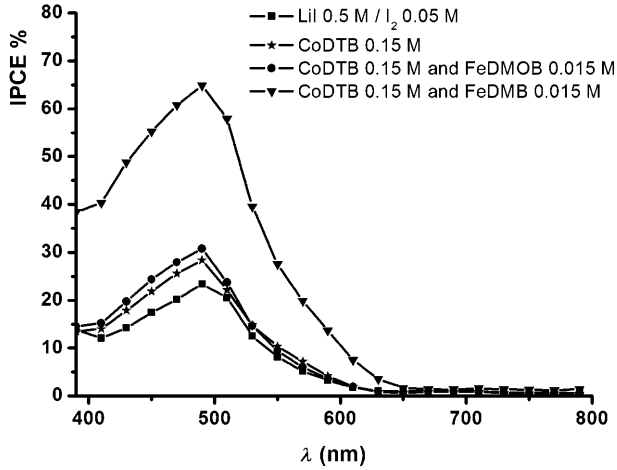

Figure 3. Photoaction spectra with various mediators in acetonitrile. $LiClO_4$ (0.5 M) was present in every electrolyte solution.

FeDMOB mixture gave slightly better results than the iodine-based system. Because both the quantum efficiency of charge injection and the light harvesting efficiency are fixed by the nature of the dye and the TiO_2, which are evidently the same in all the experiments reported here, IPCE differences can only be related to variations in the electron-collection efficiency η. The value of η depends essentially on recombination processes taking place at the TiO_2/electrolyte interface.

To rationalise this behaviour, the electron-transfer events in the presence of the different redox electrolytes were investigated by means of nanosecond laser spectroscopy ($\lambda_{excit}=532$ nm, 3 mJ pulse^{-1}). To attempt an explanation of the large differences in efficiency between I^-/I_3^-, CoDTB, and CoDTB/FeDMB, we first examined the regeneration kinetics of the dye in the presence of the reduced form of the mediators (Figure 4). As shown, all the electron donors reduce the oxidised dye on a very short time scale (6–14 ns). At this stage, the lifetime ($\tau_{2/3}$) differences are significant enough to provide a first explanation of the mediator effects on photon to electron conversion. In fact, it is evident that, despite its higher redox potential, regeneration by FeDMB (Figure 4C) is about twice as fast as that by CoTDB (Figure 4B), and its anticipated accelerating effect in the FeDMB/CoDTB mixture is actually observed (Figure 4D).

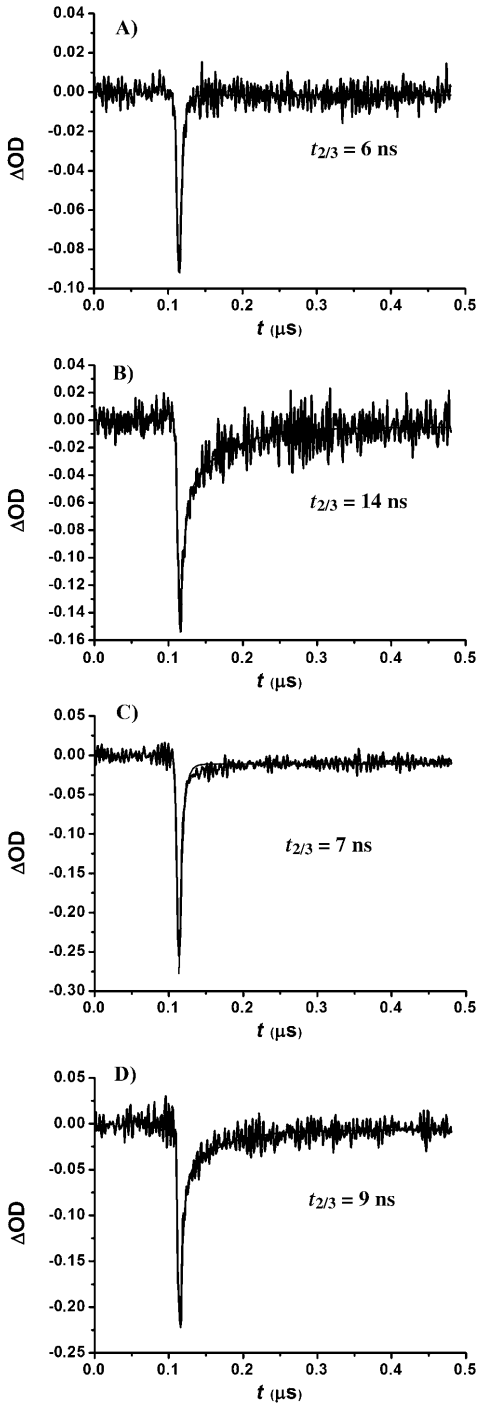

Figure 4. Transient difference absorption decays at 500 nm of dye-sensitised TiO_2 with **5** in the presence of: A: LiI (0.15 M), B: CoDTB (0.15 M), C: FeDMB (0.15 M), and D: CoDTB (0.15 M)/FeDMB (0.015 M) in acetonitrile ($\lambda_{exc}=532$ nm, $\lambda_{obs}=500$ nm; power intensity = 3 mJ pulse^{-1}). For each measurement, 0.5 M $LiCF_3SO_3$ in acetonitrile was used.

However, I^- gives the fastest reduction (Figure 4A), the results of which are essentially confined within the laser pulse. The source of the relative inefficiency of the I^-/I_3^- couple with regard to IPCE results (Figure 3) cannot reside in a sluggish Ru^{III} reduction. Recombination of TiO_2 conduction-band electrons with the oxidised mediators was, as a conse-

quence, investigated by evaluating the decay kinetics of the oxidised dye in the presence of the same concentration (0.1 M) of I_3^- and $[Co(dtb)_3]^{3+}$.[16] In the absence of the reduced form of the mediator, the only pathway of dye cation recovery is recombination with photoinjected electrons. Under these conditions, the electron recapture by the oxidised mediator would significantly lengthen the lifetime of the dye cation, because a part of the electrons is made unavailable for direct recombination.

Due to the relatively low concentration of $FeDMB^{3+}$ in the cell (which can be in the worst hypothesis only 10% vs. CoDTB) and probable fast capture by $CoDTB^{2+}$ during the regeneration process, it was not thought necessary to measure the kinetics in the presence of a steady concentration of this additional species. To avoid interference from I_3^- absorption and photochemistry,[17] the decay of dye cation absorption was monitored at 750 nm (Figure 5). The dye

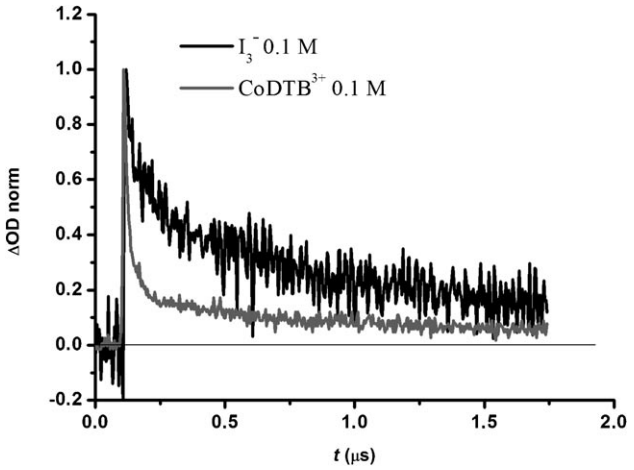

Figure 5. Recombination kinetics of photoinjected electrons in **5**-sensitised TiO_2 with oxidised mediators I_3^- (0.1 M) and $CoDTB^{3+}$ (0.1 M) in acetonitrile ($\lambda_{exc}=532$ nm, $\lambda_{obs}=750$ nm; power intensity = 14 mJ pulse^{-1}). For each measurement, 0.5 M $LiCF_3SO_3$ in acetonitrile was used.

cation recombination is much faster in the presence of $[Co(dtb)_3]^{3+}$ (70 ns) than in the presence of I_3^- (456 ns); this clearly indicates that the latter is intercepting the photoinjected electrons more efficiently. Thus, a more favourable balance between dye regeneration and recombination kinetics explains the better IPCE with CoDTB-based mediators. To further corroborate this spectral evidence, *J–V* curves were recorded under relatively low light intensities (16 mW cm^{-2}), to avoid the occurrence of mass transport limitations, which are expected in the case of bulky cobalt complexes and may conceal kinetic effects intrinsic to the electron mediator. Figure 6 (see also Supporting Information) shows that the CoDTB/FeDMB mediator clearly produces higher V_{oc} (0.32 V) than that generated by the I^-/I_3^- electrolyte (0.27 V). Considering that the $E_{1/2}$ of the Co^{II}/Co^{III} couple is about 200 mV more negative than that of I^-/I_3^-, the increased V_{oc} is explained by a considerable negative shift of the Fermi level of the TiO_2 ($\approx$250 mV) due to photoinjected electron accumulation, consistent with a decreased recombination rate in the presence of the CoDTB/FeDMB mixture.

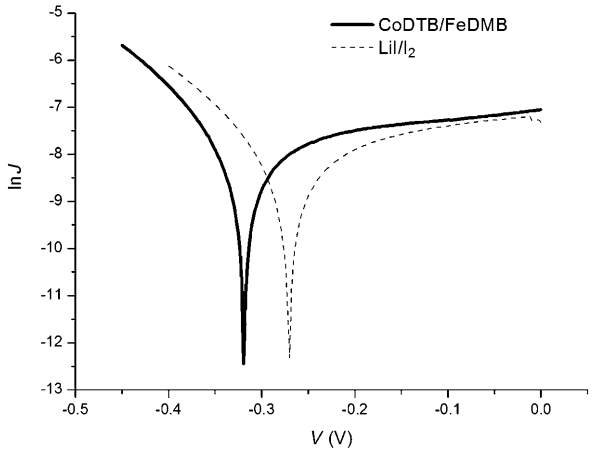

Figure 6. *J-V* curve (logarithmic) recorded under AM 1.5 G irradiation (16 mW cm^{-2}) in the presence of CoDTB/FeDMB and I^-/I_3^- mediators.

Dye **5** probably played a role in minimisation of electron recapture involving Co^{III} acceptors. Indeed, its positive charge can induce a positive polarisation at the TiO_2 surface, thus repelling Co^{III} species. Additionally, the thienyl moiety might act as a spacer, also protecting the semiconductor surface.

Another important issue that has emerged from the IPCE measurements is the dependence of the conversion efficiency on the chemical nature of co-mediators with an overall similar structure. As shown in Figure 3, 65% IPCE was obtained with CoDTB/FeDMB, whereas only 30% was observed with FeDMOB/CoDTB. Therefore, the electron-collection term is practically doubled when the bpy substituents are switched from methoxy to methyl. On the basis of the relative oxidation potentials of the Fe^{II}/Fe^{III} couples, this is not expected, because $E_{1/2ox}$ is 0.75 V and 0.85 V versus SCE for FeDMOB and FeDMB, respectively. Consequently, FeDMOB should regenerate the dye ground state even more efficiently than FeDMB, due to a larger driving force. Thus, under the hypothesis that the relevant differences between the two co-mediators could lie in recombination kinetics, the heterogeneous electron-transfer rate constant of both iron complexes on FTO substrates were estimated by applying the Nicholson method (see Supporting Information). FTO was an obvious choice for two reasons: 1) It is the material constituting the back contact of the cell, directly involved in the electron back recombination with Fe^{III} species. 2) Due to similar surface chemistry, it provides an indication of the electrochemical response of the mediator at the TiO_2 surface, which is normally too insulating at anodic potentials.

The values reported in Table 2 indicate that, whereas both heterogeneous rate constants are of the same order of magnitude, the FeDMOB results are faster. Thus, the electron recapture process by Fe^{III} could become an important mech-

Table 2. Electrochemical data obtained on FTO glass.

	$D\times10^6$ [cm^2s^{-1}][a]	$k_0\times10^4$ [$cm\,s^{-1}$] on FTO[b]	$Q_{Fe/Co}/Q_{Fe}$
FeDMOB	2.07	6.80	31
FeDMB	1.84	5.38	43

[a] Diffusion coefficient determined under Cottrell conditions; 10^{-4} M Fe complex in 0.1 M $TBAPF_6$ in acetonitrile; electrode surface area = 0.068 cm^2. [b] Electron-transfer rate constant determined at an FTO electrode in the same electrolyte.

anism of reduction of the collection efficiency, particularly in the case of inefficient reduction by Co^{II} centres (Figure 3), which would lead to a larger steady concentration of Fe^{III}.

The efficiency of Co^{II} interception was evaluated by chronocoulometry. The principle is to oxidise $FeDMB^{2+}$ or $FeDMOB^{2+}$ at the FTO electrode in the presence of a large excess of $CoDTB^{2+}$. After interception of the Co^{II} centre, the iron co-mediator is re-oxidised at the FTO surface. Because $Co(DTB)_3^{2+}$ is electrochemically inert on FTO, the number of intercepted Co^{II} centres by a given co-mediator molecule can be determined from the ratio of the charge exchanged in the presence and that exchanged in the absence of the Co^{II} excess (Figure 7, Table 2).

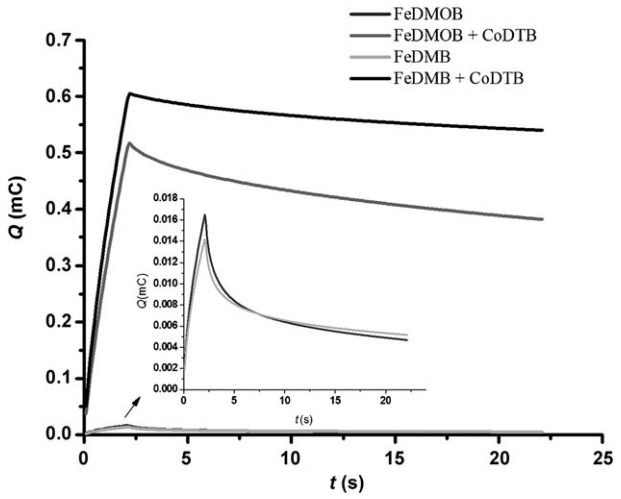

Figure 7. All experiments were conducted with a 10^{-4} M solution of FeDMOB or FeDMB and CoDTB 10^{-2} M in CH_3CN/TBAOH (0.1 M) (TBA = tetrabutylammonium). First potential step at 1.2 V for 2 s, and second potential at 0 V for 20 s.

As shown in Figure 7 and Table 2, under the same conditions, $FeDMB^{3+}$ and $FeDMOB^{3+}$ intercepted 43 and 31 Co^{II} centres, respectively. Although the chronocoulometry experiment was carried out in relatively diluted solutions, which are not strictly representative of the actual concentration profiles generated in the cell under irradiation, it still provides a useful indication: in agreement with its lower driving force for the Co^{II}–Fe^{III} electron transfer, the relative inefficiency of $FeDMOB^{3+}$ reduction may lead to a larger Fe^{III} concentration that is able to undergo recombination with photoinjected electrons at the FTO and at the TiO_2 surface. This, in addition to the faster heterogeneous electron transfer of $FeDMOB^{3+}$ compared to $FeDMB^{3+}$ leads to the relatively poor performance of the $FeDMOB^{2+/3+}$ co-mediator.

From this study, it appears that the efficiency of the dye ground-state regeneration cascade is critically dependent on the coordination sphere of the iron complex and questions the role of chemical interactions between the various species in the electrolytic medium. The low efficiency observed with FeDMOB can be a consequence of unfavourable dipole–dipole interactions between the relatively polar methoxy substituents and the *tert*-butyl groups in CoDTB, which may also lower the electronic coupling between the two redox centres. A favoured interaction between the methoxy groups and the FTO and TiO_2 surfaces through Sn^{IV} or Ti^{IV} metallic centres could also be responsible for a faster electron recapture by $FeDMOB^{3+}$, as shown by the different heterogeneous rate constants, (k_0 in Table 2).

Conclusions

We have demonstrated that a combination of an FeDMB co-mediator and a CoDTB mediator can be used to improve the electron-collection efficiency in a DSC sensitised by a (thienylterpyridine)ruthenium complex. A maximum of 65 % IPCE at 510 nm was obtained. Analogous quantum efficiency was also measured with another Ru^{II}–thienylterpyridine dye of similar structure (see Supporting Information), whereas, under the same experimental conditions, the classical I^-/I_3^- mediator gave a relatively lower performance. The charge-collection efficiency appears to be controlled by electron-transfer processes involving Fe^{III} and Co^{II} centres. The electron cascade between oxidised dye, electron mediator, and electron co-mediator, acting as a shuttle of the electronic charge, which is controllable through synthetic design, may open the possibility of improving the performance of DSCs based on noncorrosive redox couples. Additionally, the diffusional limitation of the Co^{II} electrolytes, intrinsic to the chemical nature of the mediator, could be overcome by cell engineering such as minimisation of the electrolyte layer thickness and modification of the titania substrates.

Experimental Section

Analyses and measurements: ^1H and ^{13}C NMR spectra were recorded on Bruker AC200, AC250, or DRX400 spectrometers. Electrospray mass spectra were recorded on an Agilent MSD spectrometer; CH_3CN was used as solvent. The electrochemical measurements were performed with a PST006 analytical potentiostat using a conventional single-compartment three-electrode cell. The reference electrode was the KCl calomel electrode (SCE), the working electrode a 10 mm Pt wire, and the counter electrode a 1 cm^2 vitreous carbon disc. The supporting electrolyte was 0.1 M $LiClO_4$ in CH_3CN and the solutions were purged with argon before each measurement. A 0.5 mM solution of the studied compound was generally used. All potentials are quoted versus SCE, and under these conditions the redox potential of Fc^+/Fc was 0.33 V. In all the experiments the

scan rate was 100 mV s^{-1}. Absorption UV/Vis electronic spectra were recorded on a Varian Cary E spectrometer and emission UV/Vis electronic spectra on a SLM Aminco-Bowman Series 2 apparatus; a quartz cell (1 cm × 1 cm) and deoxygenated solutions (OD < 0.05) were used. Differential excited state spectra were obtained by nanosecond transient absorption spectroscopy in acetonitrile by using the 355 nm excitation generated by a pulsed Q-switched Nd:YAG laser Continuum Surelite II (FWHM = 7 ns, 8 Hz) laser. The probe beam, orthogonal to the excitation pulse, generated by a pulsed Xe lamp was focused on an Acton Spectra Pro 2300i triple grating monochromator (5 nm band pass) and detected with a Hamamatsu R 3896 photomultiplier. Transient spectroscopy experiments on the dyed TiO_2 photoanodes were carried out with the same transient absorption apparatus. The 532 nm laser radiation was attenuated with a $KMnO_4$ chemical filter (5% T) and defocused with a plano-concave lens to obtain pulse energies of the order of 3 mJ cm^{-2}. To obtain a satisfactory S/N ratio, oscilloscope traces were averaged over 10 laser shots. To avoid direct TiO_2 excitation, the analysis beam was filtered from its UV component by using a 400 nm cut-off filter. No sample degradation was observed over several laser shots Oscillographic traces were acquired on a Lecroy 9360 600 MHz oscilloscope and transferred to a personal computer by means of a custom-made labVIEW program. IPCE measurements were performed by illumination of the cell using an Osram 150 W Xenon lamp coupled to an Applied Photophysics monochromator. The irradiated surface was 0.5 cm^2. Photocurrents were measured under short circuit conditions by a digital Agilent 34401A multimeter. Incident irradiance was measured with a 1 cm^2 Centronic OSD100-7Q calibrated silicon photodiode. *J-V* curves were recorded under AM 1.5 G by linearly sweeping the potential with a scan speed of 10 mV s^{-1} by using an EcoChemie PGSTAT 302/N potentiostat. Potential step experiments were performed with the same apparatus described above, by stepping the potential between 1.2 and 0 V versus SCE. The electrochemical experiments aimed at the determination of the heterogeneous electron-transfer rate constant were conducted in a three-electrode cell equipped with a Luggin capillary to minimise the IR drop across the cell.

TiO_2 electrode preparation:[6] TiO_2 colloidal paste was prepared by hydrolysis of Ti^{IV} isopropoxide. The nanocrystalline TiO_2 photoelectrodes were prepared by depositing the paste onto transparent conducting FTO glass (Hartford TEC 8 8 Ω per square) according to the well-known "Scotch tape" method. The thin films were allowed to dry at room temperature for 20 min and finally fired at 450 °C for 40 min. The still hot electrodes were immersed in the dye solution and kept at 80 °C for 5 h, after which the absorption was deemed complete. The efficiency of absorption was evaluated by UV/Vis spectroscopy: photoelectrodes characterised by an optical density ≥1 at the MLCT maximum of the sensitiser were commonly obtained. Dye solutions were prepared by dissolving a small amount of the Ru^{II} complex in acetonitrile (ca. 4 mg in 10 mL solvent). The solutions were sonicated and filtered to remove suspended undissolved dye.

Counter electrode preparation: Platinum-coated counter electrodes were obtained by spraying a 5×10^{-3} M H_2PtCl_6 (Fluka) solution in isopropyl alcohol on the well-cleaned surface of an FTO glass. This procedure was repeated 5–10 times to obtain a homogeneous distribution of H_2PtCl_6 droplets. The electrodes were dried under gentle air flow and treated in an oven at 380 °C for 15 min, to result in the formation of stable platinum clusters. Gold-coated electrodes, used with cobalt-based mediators, were obtained by thermal vapour deposition on FTO of a 5–7 nm thick chromium adhesion layer followed by a 30–35 nm thick gold layer. The average pressure of the vacuum chamber of the evaporator was ca. 9×10^{-6} Torr.

Photoelectrochemical cell assembly:[6] Parafilm-sealed cells were constructed by pressing the sensitised photoanode against a counter electrode equipped with a Parafilm frame used to confine the liquid electrolyte inside the cell. The thickness of the liquid layer corresponded roughly to the thickness of the frame borders (≈120 μm). In this configuration, the cell was stable towards solvent evaporation and leaking for several days even when volatile solvents such as acetonitrile were used. In both cases, metallic clamps were used to hold the two electrodes firmly together.

Preparation of FeDMB, FeDMOB, and CoDTB mediators and terpyridines 1 and 3: The FeDMB, FeDMOB, and CoDTB mediators[6,9] and terpyridines **1** and **3**[18,19] were prepared according to previously published procedures.

Preparation of complex 4: A mixture of ligand **1** (250 mg, 0.79 mmol) and $RuCl_3 \cdot xH_2O$ (230 mg, 0.87 mmol) in ethanol (20 mL) was heated at reflux under argon for 3 h. After cooling of the mixture, the solid was collected by filtration and washed thoroughly with ethanol and diethyl ether; this yielded **2** quantitatively. Complex **2** (50 mg, 0.09 mmol) was then mixed with $AgBF_4$ (57 mg, 0.29 mmol) in DMF (10 mL), and the solution was heated at reflux for 3 h. After cooling of the mixture, AgCl was removed by filtration over a Celite pad. The filtrate was then transferred to an argon-flushed flask and brought to reflux. A solution of ligand **3** (30 mg, 0.09 mmol) in DMF (10 mL) was then added dropwise over 10 min. After the end of the addition, the mixture was heated at reflux for 3 h. After cooling of the mixture, the solvent was removed by evaporation and the residue was dissolved in a minimal amount of acetone. Saturated aq KPF_6 (20 mL) was added and the acetone was removed by evaporation to give a precipitate, which was washed with distilled water and diethyl ether and finally dried under reduced pressure. After column chromatography (silica gel, acetone/water/sat. aq $NaNO_3$ 70:30:1), **4** was obtained. Yield: 51%; ^{1}H NMR (CD_3CN): $\delta = 8.98$ (s, 2H), 8.95 (s, 2H), 8.61–8.52 (m, 4H), 8.42–8.33 (m, 1H), 8.01–7.95 (m, 2H), 7.92–7.84 (m, 4H), 7.81–7.76 (m, 1H), 7.59–7.50 (m, 1H), 7.40–7.35 (m, 4H), 7.15–6.99 (m, 4H), 6.84–6.75 ppm (m, 1H); MS (ES): *m*/*z*: 861.1 $[M-PF_6]^+$, 724.1 $[M-2PF_6]^+$, 357.9 $[M-2PF_6]^{2+}$.

Preparation of dye 5: $KMnO_4$ (93 mg, 0.58 mmol) and a mixture of acetonitrile and water (10 mL each), previously adjusted to pH 14 (KOH), were added to **4** (45 mg, 0.045 mmol). The reaction mixture was stirred for 24 h at RT. The excess $KMnO_4$ was then destroyed with sodium thiosulfate, the solution was filtered through a Celite pad, and the solid was washed with acetonitrile. After acidification of the mixture (pH 3, diluted HCl), KPF_6 (1.07 g) was added. The acetonitrile was finally evaporated and the residue was washed with water and diethyl ether and dried. After column chromatography (silica gel, acetone/water/sat. aq $NaNO_3$ 70:30:1), **5** was obtained. Yield: 51%; ^{1}H NMR (CD_3CN): $\delta = 9.27$ (s, 2H), 8.90 (s, 2H), 8.60–8.49 (m, 4H), 8.20–8.12 (m, 1H), 7.88–7.77 (m, 5H), 7.36–7.29 (m, 5H), 7.11–7.02 ppm (m, 4H). MS (ES): *m*/*z*: 693.0 $[M-2PF_6]^+$, 649.1 $[M-COOH-2PF_6]^+$, 346.9 $[M-2PF_6]^{2+}$, 324.5 $[M-COOH-2PF_6]^{2+}$.

Acknowledgements

The authors thank the CNRS and French Ministry of Research for support. Funding from Polo Solare Organico Regione Lazio is gratefully acknowledged. The authors also thank the technical assistance of Mr. Sandro Fracasso.

[1] a) A. Juris, V. Balzani, F. Barigelletti, S. Campagna, P. Belser, A. von Zelewsky, *Coord. Chem. Rev.* **1988**, *84*, 85–277; b) B. O'Regan, M. Grätzel, *Nature* **1991**, *353*, 737–740; c) A. Hagfeldt, M. Grätzel, *Chem. Rev.* **1995**, *95*, 49–68; d) M. K. Nazeeruddin, S. Zakeeruddin, J.-J. Lagref, P. Liska, P. Comte, C. Barolo, G. Viscardi, K. Schenk, M. Graetzel, *Coord. Chem. Rev.* **2004**, *248*, 1317–1328; e) N. Robertson, *Angew. Chem.* **2006**, *118*, 2398–2405; *Angew. Chem. Int. Ed.* **2006**, *45*, 2338–2345.

[2] a) C. Nasr, S. Hotchandani, P. V. Kamat, *J. Phys. Chem. B* **1998**, *102*, 4944–4951; b) M. Grätzel, *Pure Appl. Chem.* **2001**, *73*, 459–467.

[3] H. Nusbaumer, S. M. Zakeeruddin, J.-E. Moser, M. Grätzel, *Chem. Eur. J.* **2003**, *9*, 3756–3763.

[4] a) B. C. O'Regan, K. Walley, M. Juozapavicius, A. Anderson, F. Matar, T. Ghaddar, S. M. Zakeeruddin, C. d. Klein, J. R. Durrant, *J. Am. Chem. Soc.* **2009**, *131*, 3541–3548; b) B. C. O'Regan, I. Lopez-Duarte, M. V. Martinez-Diaz, A. Forneli, J. Albero, A. Morandeira, E. Palomares, T. Torres, J. R. Durrant, *J. Am. Chem. Soc.* **2008**, *130*,

2906–2907; c) J. M. Gardner, J. M. Giaimuccio, G. J. Meyer, *J. Am. Chem. Soc.* **2008**, *130*, 17252–17253.
[5] a) H. Nusbaumer, J.-E. Moser, S. M. Zakeeruddin, M. K. Nazeeruddin, M. Grätzel, *J. Phys. Chem. B* **2001**, *105*, 10461–10464; b) P. J. Cameron, L. M. Peter, S. M. Zakeeruddin, M. Grätzel, *Coord. Chem. Rev.* **2004**, *248*, 1447–1453.
[6] S. A. Sapp, C. M. Elliott, C. Contado, S. Caramori, C. A. Bignozzi, *J. Am. Chem. Soc.* **2002**, *124*, 11215–11222.
[7] J. J. Nelson, T. J. Amick, C. M. Elliott, *J.Phys. Chem. C* **2008**, *112*, 18255–18263.
[8] C. M. Elliott, S. Caramori, C. A. Bignozzi, *Langmuir* **2005**, *21*, 3022–3027.
[9] S. Cazzanti, S. Caramori, R. Argazzi, C. M. Elliott, C. A. Bignozzi, *J. Am. Chem. Soc.* **2006**, *128*, 9996–9997.
[10] S. Caramori, S. Cazzanti, L. Marchini, R. Argazzi, C. A. Bignozzi, D. Martineau, P. C. Gros, M. Beley, *Inorg. Chim. Acta* **2008**, *361*, 627–634.
[11] a) J. Hjelm, E. C. Constable, E. Figgemeier, A. Hagfeldt, R. Handel, C. E. Housecroft, E. Mukhtar, E. Schofield, *Chem. Commun.* **2002**, 284–285; b) S. Encinas, L. Flamigni, F. Barigelletti, E. C. Constable, C. E. Housecroft, E. R. Schofield, E. Figgemeier, D. Fenske, M. Neuburger, J. G. Vos, M. Zehnder, *Chem. Eur. J.* **2002**, *8*, 137–150.
[12] C. Houarner-Rassin, E. Blart, P. Buvat, F. Odobel, *J. Photochem. Photobiol. A* **2007**, *186*, 135–142.
[13] a) A. J. Mozer, Y. Wada, K. J. Jiang, N. Masaki, S. Yanagida and S. N. Mori, *Appl. Phys. Lett.* **2006**, *89*, 043509; b) V. Aranyos, A. Hagfeldt, H. Grennberg, E. Figgemeier, *Polyhedron* **2004**, *23*, 589–598.
[14] E. Figgemeier, V. Aranyos, E. C. Constable, R. W. Handel, C. E. Housecroft, C. Risinger, A. Hagfeldt, E. Mukhtar, *Inorg. Chem. Commun.* **2004**, *7*, 117–121.
[15] C. Houarner-Rassin, F. Chaignon, C. She, D. Stockwell, E. Blart, P. Buvat, T. Lian, F. Odobel, *J. Photochem. Photobiol. A* **2007**, *192*, 56–65.
[16] A. Grabulosa, D. Martineau, M. Beley, P. C. Gros, S. Cazzanti, S. Caramori, C. A. Bignozzi, *Dalton Trans.* **2009**, 63–70.
[17] A transient positive absorption, with a lifetime of hundreds of nanoseconds, could be observed at 500 nm upon 532 nm laser excitation of an I_3^- solution in acetonitrile.
[18] J. Husson, M. Beley, G. Kirsch, *Tetrahedron Lett.* **2003**, *44*, 1767–1770.
[19] J. Husson, E. Migianu, M. Beley, G. Kirsch, *Synthesis* **2004**, 267–270.

Received: October 6, 2009
Published online: January 13, 2010

